Unsteady solute dispersion in Bingham fluid flow with combined effects of wall absorption, magnetic field and electric field

Suchita T.S [1], S Senthamilselvi[1] and R. VijayaKumar[2]

[1]*Department of Mathematics,*
Vels Institute of Science, Technology & Advanced Studies,Tamil Nadu, India.
[2]*Mathematics Section, FEAT, Annamalai University, Annamalainagar-608002,India.*
Department of Mathematics, Periyar Government Arts College, Cuddalore,
TamilNadu – 607 001, India.
Email:[1]chiku2712@gmail.com, [2]rathirath_viji@yahoo.co.in
Corresponding author Email: [1]msselvi2305@gmail.com

KEYWORDS

Bingham fluid, wavy channel, interphase mass transfer, Generalized dispersion model.

ABSTRACT

The objective of the present investigation is to disseminate a solute at the boundary wavy walls of the parallel channel while it is undergoing an irreversible first-order chemical reaction. This rheological characteristic, which results from suspension in the fluid, influences the dispersion and convection coefficients. The exchange coefficient, which is independent of the solvent fluid velocity, is primarily caused by the interphase mass transfer. Additionally impacted by the wall-catalyzed process are the convection and dispersion coefficients. Solute dispersion can be studied to understand how medications or nutrients are transferred in plasma during blood flow via porous surfaces. Beyond absorption, circulatory flow is a vital component. Our results demonstrate that wavy wall absorption significantly affects transport coefficients.

1. Introduction

In physiological situations where a first-order chemical reaction takes place at the tube wall, interphase mass transfer can be used. Transporting oxygen and nutrients to tissue cells and extracting metabolic waste products from tissue cells are two examples of such circumstances. It also occurs in the pulmonary capillaries, where the blood absorbs oxygen and carbon dioxide is expelled. Many studies on the fluid dynamics of biological fluids under the influence of magnetic fields have been conducted in the past ten years. The lack of biocompatibility of smooth (rough) surfaces in metal-implanted or extracorporeal artificial organs results in a variety of blood injury types. It is dangerous since they create stress that results in force. Eventually, this force affects the red blood cells, or erythrocytes, causing haemolysis, or the loss of haemoglobin. Several authors focused on dispersion to understand the transport of nutrients in blood and different artificial devices (Middleman (1972), Lightfoot (1974), Cooney (1976), Jayaraman et al., (1981)). The effective dispersion coefficient was examined in relation to the average flow speed, the tube radius, and the molecular diffusion coefficient by Taylor (1953, 1954), who investigated the dispersion process in Newtonian flow. Sankarasubramanian and Gill (1973) explored the dispersion of a non-uniform initial distribution in time-variable isothermal laminar flow in a tube with a first-order rate process near the tube wall. Through a precise process, they investigated miscible dispersion in laminar flow in a tube with interfacial transport caused by an irreversible first-order reaction at the tube wall. The exchange coefficients are a novel idea, and a generic formula demonstrating their time-dependent character is constructed. Finding the average concentration distribution in terms of tabular functions is made possible by the exchange coefficient, which represents the interphase process. Only the scenario of dispersion in a fully established steady flow was included in the analysis. Siddheshwar et al. (2000) have studied the problem of plane-Poiseuille flow of a power law fluid with interphase mass transfer. Using the generalised dispersion model of Sankarasubramanian and Gill (1970), Nirmala P. Ratchagar and Vijaya Kumar (2015) examined the impact of couple stress and magnetic field on unstable convective diffusion with interphase mass transfer. In the simplest scenario, they take into account a first order chemical reaction at the walls during an exact analysis of unsteady convection in couple stress fluid flows. Reaction at the walls is of practical interest. The exact analysis of miscible solute dispersion with interphase mass transfer in a couple stress poorly conducting fluid surround by porous beds was examined by Rudraiah et al. (2016). The exchange coefficient, convective coefficient, and dispersion coefficient are highlighted by the utilization the generalised dispersion model of Sankarasubramanian and Gill (1973). The porosity parameter and couple stress parameter resulting from suspension in the fluid only affect the final two coefficients. The interphase mass transfer is the primary cause of the exchange coefficient, which is unaffected by the solvent fluid velocity. The convection and dispersion coefficients are also impacted by the interphase mass transfer.

Siti Nurul Aifa Mohd Zainul Abidin (2024) explored the Herschel-Bulkley (H-B) fluid model, a non-Newtonian mathematical model of blood flow in a catheterised stenosed artery. Additionally, the wall absorption effect is taken into account in this inquiry. The convective-diffusion equation that describes the dispersion process determines the solute movement. Three effective transport coefficients exchange, convection, and diffusion are obtained by solving the transport equation using an accurate technique known as the Generalised Dispersion Model (GDM). The goal of this work has been to examine the flow properties of a Bingham plastic fluid through a porous material when both an electric and magnetic field are present. In order to emphasise the dispersion coefficient and mean concentration, the generalised dispersion model of Sankarasubramanian and Gill (1970) has been applied. convection coefficient and dispersion coefficient are affected by the rheological parameter, magnetic field, electric number and porous parameter arising due to suspension in the fluid. The exchange coefficient arises mainly due to the interphase mass transfer, and it is independent of the solvent fluid velocity. The convection and dispersion coefficients are also affected by the interphase mass transfer. Finally the outcome of non-dimensional parameter is deliberated by graphs.

2. Mathematical Formulation

The constitutive equation for blood, expressed as Bingham fluid, is as follows, according to Misra and Adhikary (2017)

$$\tau_{xy} = -\mu_0 \frac{\partial u_f^*}{\partial y} \pm \tau_0 \qquad if \qquad |\tau_{xy}| > \tau_0 \tag{1}$$

$$\frac{\partial u_f^*}{\partial y} = 0 \qquad if \qquad |\tau_{xy}| < \tau_0 \tag{2}$$

In the channel, equations (1) and (2) depict the two stages of blood flow. The flat velocity profile in the central core region creates the plug flow region. Shear stress in this plug flow zone is less than yield stress τ_0.

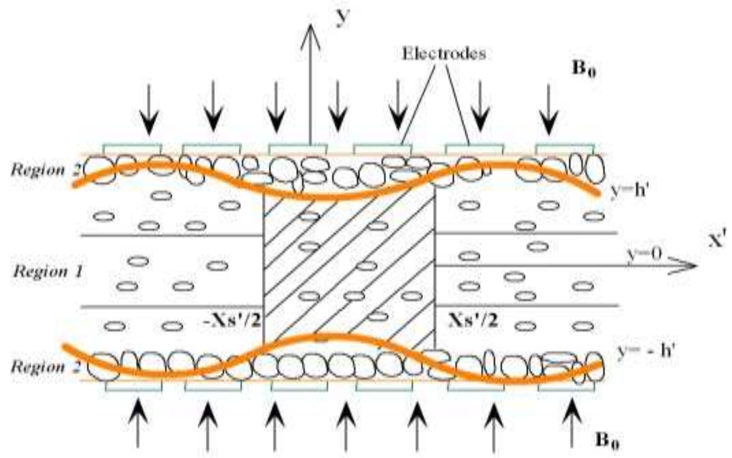

Figure 1: Physical problem

The following assumptions are used to obtain the governing equations along with associated boundary conditions:

An electric field and a uniform magnetic field B_0 are supplied to the blood flow in the y-direction. In a channel enclosed by porous beds, the solute diffuses over the porous medium in a fully formed flow. The horizontal channel two side wall are at $y = h' = d + a\cos\lambda x'$ and $y = -h' = -d - a\cos\lambda x'$. For concentration C, which depends on coordinates x' and y and time (t), a slug is added. The mass balance equation concerning the solute concentration C with heterogeneous chemical reaction. Under the aforementioned presumption, the following governing equations apply to the incompressible flow of a non-Newtonian fluid in cartesian coordinates:

Region 1:

$$\frac{\partial u_f^*}{\partial x'} = 0 \qquad (3)$$

$$-\frac{\partial p'}{\partial x'} + \mu\frac{\partial \tau_{xy}}{\partial y} - \frac{\mu}{k}u_f^* - B_0^2\sigma_0 u_f^* + \rho_e E_x = 0 \qquad (4)$$

$$-\frac{\partial p'}{\partial y} + \rho_e E_y = 0 \qquad (5)$$

The concentration C satisfying the convective diffusion equation gives

$$\frac{\partial C}{\partial t} + u_f^*\frac{\partial C}{\partial x'} = D\left(\frac{\partial^2 C}{\partial x'^2} + \frac{\partial^2 C}{\partial y^2}\right) \qquad (6)$$

Region 2:

$$\frac{\partial u_p^*}{\partial x} = 0 \qquad (7)$$

$$-\frac{\partial p'}{\partial x'} - \frac{\mu}{k}u_p^* + -B_0^2\sigma_0 u_p^* + \rho_e E_x + \alpha_0 = 0 \qquad (8)$$

$$-\frac{\partial p'}{\partial y} + \rho_e E_y = 0 \qquad (9)$$

Boundary conditions for velocity and concentration are

$$\frac{\partial u_f^*}{\partial y} = -\frac{\alpha}{\sqrt{k}}(u_f^* - u_p^*) \quad at \quad y = h' \qquad (10)$$

$$\frac{\partial u_f^*}{\partial y} = \frac{\alpha}{\sqrt{k}}(u_f^* - u_p^*) \quad at \quad y = -h' \qquad (11)$$

The symmetric conditions,

$$\frac{\partial u_f^*}{\partial y} = 0 \qquad at \qquad y = 0 \tag{12}$$

$$u_f^* = u_{pf}^* \qquad at \qquad y = y_c \tag{13}$$

$$C' = C_0' \psi_1(x') Y_1(y) \qquad at \qquad t = 0 \tag{14}$$

$$\left.\begin{aligned} -D\frac{\partial C'}{\partial y}(t, x', h') &= K_s C' \\ D\frac{\partial C'}{\partial y}(t, x', -h') &= K_s C' \end{aligned}\right\} \tag{15}$$

As the amount of solute in the system is finite,

$$C'(t, \infty, y) = \frac{\partial C'}{\partial x'}(t, \infty, y) = 0 \tag{16}$$

where, u_f^* - component of velocity, p^*-pressure, μ-viscosity of the fluid, B_0- applied magnetic field, σ_0- the electrical conductivity, t -time, D -molecular diffusivity, k-permeability of the porous medium, u_p^* -Darcy velocity, α-slip parameter, C_0'-reference concentration, Ks-reaction rate constant catalyzed by the walls, τ_{xy} -shear stress, μ_0-plastic dynamic viscosity, τ_0-yield stress. Beavers and Joseph's (1967) slip condition at the lower and upper permeable surfaces is represented by equations (10) and (11).

Introducing the non-dimensional quantities

$$U_f = \frac{u_f^*}{u'}, U_p = \frac{u_p^*}{u'}, \eta = \frac{y}{d}, X' = \frac{x'}{d\,Pe}, X'_s = \frac{x'_s}{d\,Pe}, Pe = \frac{u'd}{D}, p^* = \frac{p}{\rho u'^2}, \tau = \frac{Dt}{d^2}, \theta = \frac{C'}{C_0},$$

$$\beta = \frac{k_s d}{D}, \rho_e = \frac{\hat{\rho}_0 d^2}{\in_0 V}, E'_x = \frac{E_x d}{V}, h = \frac{h'}{d}$$

In non-dimensional form, equations (3) to (9) are

Region 1:

$$\frac{d^4 U_f}{\partial \eta^4} - M^2 U_f = s_2 + We\, s_1(1 - \alpha_c \eta) \tag{17}$$

$$\frac{\partial \theta}{\partial \tau} + U_f \frac{\partial \theta}{\partial X'} = \frac{1}{Pe^2}\left(\frac{\partial^2 \theta}{\partial X'^2} + \frac{\partial^2 \theta}{\partial \eta^2}\right) \tag{18}$$

we define the axial coordinate moving with the average velocity of flow as $x = x' - tu'$ which is in dimensionless form $X = X' - \tau$.Then equation (13) becomes

$$\frac{\partial \theta}{\partial \tau} + U_f' \frac{\partial \theta}{\partial X} = \frac{1}{Pe^2}\left(\frac{\partial^2 \theta}{\partial X^2} + \frac{\partial^2 \theta}{\partial \eta^2}\right) \tag{19}$$

where, $U_f' = \frac{U_f}{\bar{U}_f}$

Region 2:

$$U_p = -\frac{\left[\frac{\mathrm{Re}}{Pe} + We\, s_1(1 - \alpha_c \eta)\right]}{\sigma^2 + M^2} \tag{20}$$

The dimensionless form of the initial and boundary conditions (10) to (16)

$$\frac{\partial U_f}{\partial \eta} = -\alpha\sigma(U_f - U_p) \qquad at \qquad \eta = h \tag{21}$$

$$\frac{\partial U_f}{\partial \eta} = \alpha\sigma(U_f - U_p) \qquad at \qquad \eta = -h \tag{22}$$

$$\frac{\partial U_f}{\partial \eta} = 0 \qquad at \qquad \eta = 0 \tag{23}$$

$$U_f = U_{pf} \qquad at \qquad \eta = \eta_c \tag{24}$$

$$\theta = \psi(X) Y(\eta) \qquad at \qquad \tau = 0 \tag{25}$$

$$\left.\begin{aligned} \frac{\partial \theta}{\partial \eta}(\tau, X, h) &= -\beta\theta \\ \frac{\partial \theta}{\partial \eta}(\tau, X, -h) &= \beta\theta \end{aligned}\right\} \tag{26}$$

$$\theta(\tau, \infty, \eta) = \frac{\partial \theta}{\partial X}(\tau, \infty, \eta) = 0 \tag{27}$$

where $M^2 = \dfrac{B_0^2 \sigma_0 d^2}{\mu}$ is the square of the Hartmann number, $We = \dfrac{\varepsilon_0 V^2}{\mu_0}$ is the electric numbers $P = -\dfrac{\text{Re}}{Pe}\dfrac{\partial p}{\partial X'}$, $\text{Re} = \dfrac{\rho u' d}{\mu}$ is the Reynolds number, $Pe = \dfrac{u' d}{D}$ is the Peclet number, $\sigma = \dfrac{d}{\sqrt{k}}$ is the porous parameter, K_s is the reaction rate constant catalyzed by the walls.

3. Method of solution

By solving equation (17) and satisfying the boundary conditions (21) to (24). The blood velocity is obtained as

$$U_f = \begin{cases} A_1 e^{M\eta_c} + A_2 e^{-M\eta_c} - \dfrac{1}{M^2} We \;\; s_1(1-\alpha_c \eta_c), \; if \;\; 0 < \eta \le \eta_c \\ A_1 e^{M\eta} + A_2 e^{-M\eta} - \dfrac{1}{M^2} We \;\; s_1(1-\alpha_c \eta), \; if \;\; \eta_c < \eta \le h \end{cases} \tag{28}$$

$$where, \; A_1 = \frac{s_5 + s_4 A_2}{s_3}, A_2 = \frac{s_5 + \dfrac{s_3}{M} We\, s_1 \alpha_c}{s_3 - s_4}$$

$$s_1 = \frac{X_0 \alpha_c Pe}{2}, s_2 = \frac{\text{Re}}{Pe}\frac{\partial p}{\partial \xi}, s_3 = (M + \alpha\sigma)e^{hM}, s_4 = (M - \alpha\sigma)e^{-hM}$$

$$s_5 = \frac{We\, s_1}{M^2}\left(\alpha\sigma(1-\alpha_c h) - \alpha_c\right) + \alpha\sigma U_p, U_p = -\frac{1}{\sigma^2 + M^2}\left(\frac{\text{Re}}{Pe} + We\, s_1(1-\alpha_c h)\right)$$

The axial velocity components that have been normalised are

$$U_f' = \frac{U_f}{\bar{U}_f} \tag{29}$$

where

$$\bar{U}_f = \frac{1}{h}\int_0^h U_f(\eta) d\eta \tag{30}$$

$$= \frac{1}{2hM} e^{-M(h+\eta_c)}\left(-2A_2 e^{M\eta_c} + 2A_2 e^{hM}(1 + M\eta_c) + e^{(h+\eta_c)M}(s_1 We(h(-2 + h\alpha_c) + \alpha_c \eta_c^2\right) + 2A_1(e^{hM} + e^{M\eta_c}(-1 + M\eta_c))))$$

The generalised dispersion model of Gill and Sankarasubramanian (1970), which is expressed as a series expansion in the form of

$$\theta(\tau, X, \eta) = \theta_m(\tau, X) + f_1(\tau, \eta)\frac{\partial \theta_m}{\partial X} + f_2(\tau, \eta)\frac{\partial^2 \theta_m}{\partial X^2} + \ldots \tag{31}$$

where, θ_m is the dimensionless cross sectional average concentration, given by

$$\theta(\tau, X) = \frac{1}{h}\int_0^h \theta(\tau, X, \eta) d\eta \tag{32}$$

Integrating equation (19) with respect to η in (0,h) and using the equation (31) and (32), we get

$$\frac{\partial\theta_m}{\partial\tau}=\frac{1}{Pe^2}\frac{\partial^2\theta}{\partial X^2}-\frac{1}{h}\frac{\partial}{\partial X}\int_0^h U_f'\left(\theta_m(\tau,X)+f_1(\tau,\eta)\frac{\partial\theta_m}{\partial X}+f_2(\tau,\eta)\frac{\partial^2\theta_m}{\partial X^2}+...\right)d\eta \quad (33)$$

In this model we write

$$\frac{\partial\theta_m}{\partial\tau}=\sum_{k=0}^{\infty}K_k(\tau)\frac{\partial^k\theta}{\partial X^k} \quad (34)$$

where the dispersion coefficient, $K_k(\tau)$ Substituting the Equation (34) in (33) we obtain

$$K_0\theta_m+K_1(\tau)\frac{\partial\theta}{\partial X}+K_2(\tau)\frac{\partial^2\theta}{\partial X^2}+K_3(\tau)\frac{\partial^3\theta}{\partial X^3}+......=\frac{1}{Pe^2}\frac{\partial^2\theta}{\partial X^2}+\left(\frac{\partial}{\partial\eta}(f_0\theta_m+f_1\frac{\partial\theta_m}{\partial X})\right)_0^h$$
$$-\frac{1}{h}\frac{\partial}{\partial X}\int_0^h U_f'\left(f_0(\tau,\eta)\theta_m(\tau,X)+f_1(\tau,\eta)\frac{\partial\theta_m}{\partial X}+f_2(\tau,\eta)\frac{\partial^2\theta_m}{\partial X^2}+...\right)d\eta$$

Equating the coefficient $\frac{\partial\theta_m}{\partial X},\frac{\partial^2\theta_m}{\partial X^2},...,$.we get,

$$K_i(\tau)=\frac{\delta_{ij}}{Pe^2}+\frac{1}{2}\frac{\partial f_i}{\partial X}(\tau,1)-\frac{1}{h}\int_0^h U_f'f_{i-1}(\tau,\eta)d\eta \qquad (i=1,2,3,....) \quad (35)$$

where $f_{-1}=0$

Equation (35) can be truncated after the term involving K_2 without causing serious error, because $K_3, K_{4,}$, etc. become negligibly small compared to K_2.

The resulting model for the mean concentration is

$$\frac{\partial\theta_m}{\partial\tau}=K_0\theta_m+K_1(\tau)\frac{\partial\theta}{\partial X}+K_2(\tau)\frac{\partial^2\theta}{\partial X^2} \quad (36)$$

The differential equations of the following form are obtained by substituting (31) in (19) and using generalised dispersion model of Gill and Sankarasubramanian (1973) to the resultant equation.

$$\frac{\partial f_k}{\partial\tau}=\frac{\partial^2 f_k}{\partial\eta^2}-U_f'f_{k-1}+\frac{1}{Pe^2}f_{k-2}=\sum_{i=0}^{k}K_i f_{k-i} \qquad (k=0,1,2,...) \quad (37)$$

where, $f_{-1}=f_{-2}=0$

Since θ_m is chosen to satisfy the initial and boundary conditions on θ from equations (25) to (26) conditions on the f_k function becomes

$$f_k=finite \quad at \quad \tau=0 \quad (38)$$

$$\frac{\partial}{\partial\eta}f_k(\tau,h)=-\beta f_k \quad (39)$$

$$\frac{\partial}{\partial\eta}f_k(\tau,0)=0 \quad (40)$$

Also, from equation (32) we have

$$\frac{1}{h}\int_0^h f_k(\tau,\eta)d\eta=\delta_{k0},(k=0,1,2) \quad (41)$$

Substituting k = 0 in equation (37) we get the differential equation for f_0 as

$$\frac{\partial f_0}{\partial\tau}=\frac{\partial^2 f_0}{\partial\eta^2}-f_0K_0 \quad (42)$$

For i = 0 in (30) we have

$$K_0(\tau)=\left(\frac{\partial f_0}{\partial\eta}\right)_0^h-f_0K_0 \quad (43)$$

These two equations (42) and (43) must be solved simultaneously, with an initial condition for using (32) that requires entering that equation to obtain

$$\theta_m(0,X)=\frac{1}{h}\int_0^h \theta_m(0,X,\eta)d\eta \tag{44}$$

Substituting $\tau=0$ in (31) and setting $f_k(\eta)=0\,(k=1,2,3)$ gives the initial condition for f_0 as

$$f_0(0,\eta)=\frac{\theta(0,X,\eta)}{\theta_m(0,X)} \tag{45}$$

Substituting equation (39) and (40) into equation (45),we get

$$f_0(0,\eta)=\frac{\psi(\eta)}{\frac{1}{h}\int_0^h \psi(\eta)d\eta} \tag{46}$$

The solution of the reaction diffusion equation (42) with these conditions are formulated as

$$f_0(\tau,\eta)=g_0(\tau,\eta)\exp\left[-\int_0^h K_{0I}(\eta)d\eta\right] \tag{47}$$

from which it follows that $g_0(\tau,\eta)$ has to satisfy

$$\frac{\partial g_0}{\partial\tau}=\frac{\partial^2 g_0}{\partial\eta^2} \tag{48}$$

with conditions

$$f_0=g_0=\frac{\psi(\eta)}{\frac{1}{h}\int_0^h \psi(\eta)d\eta} \quad at \quad \tau=0 \tag{49}$$

$$g_0=finite \quad at \quad \eta=0 \tag{50}$$

$$\frac{\partial g_0}{\partial\eta}=-\beta g_0 \quad at \quad \eta=h \tag{51}$$

The solution of (48) subject to conditions (49) to (51) is

$$g_0(\tau,\eta)=\sum_{n=0}^{\infty}A_n e^{-\mu_n^2\tau}Cos(\mu_n\eta) \tag{52}$$

where μ_n's are the roots of

$$\mu_n\tan\mu_n=\beta,\quad n=0,1,2,... \tag{53}$$

And A_n 's are given by

$$A_n=\frac{\int_0^h \psi(\eta)\cos\mu_n\eta\, d\eta}{\left(1+\frac{\sin 2\mu_n}{2\mu_n}\right)\int_0^h \psi(\eta)d\eta} \tag{54}$$

From (47), it follows that

$$f_0(\tau,\eta)=\frac{2g_0(\tau,\eta)}{\int_0^h g_0(\tau,\eta)d\eta}=\frac{\sum_{n=0}^{\infty}A_n e^{-\mu_n^2\tau}Cos(\mu_n\eta)}{\sum_{n=0}^{\infty}\frac{A_n}{\mu_n}e^{-\mu_n^2\tau}Sin\,\mu_n} \tag{55}$$

MATHEMATICA 12.0 is used to obtain the first ten roots of the transcendental equation (53), which are listed in Table 1. In the expansions of and, these 10 roots ensure the series will converge. With that, we obtain from (48) in the form

$$K_0(\infty)=\frac{\sum_{n=0}^{\infty}A_n\mu_n e^{-\mu_n^2\tau}Sin(\mu_n\eta)}{\sum_{n=0}^{\infty}\frac{A_n}{\mu_n}e^{-\mu_n^2\tau}Sin\,\mu_n} \tag{56}$$

Here $K_0(\tau)$ is independent of velocity distribution.

As $\tau \to \infty$, we get the asymptotic solution for K_0 from (56) as

$$K_0(\infty) = -\mu_0^2 \quad (57)$$

where μ_0 is the first root of the equation (53). Physically, this represents first order chemical reaction coefficient to obtain $K_0(\infty)$. We get $K_1(\infty)$, from (35) (with i = 1) knowing $f_0(\infty,\eta)$ and $f_1(\infty,\eta)$. Likewise, $K_2(\infty), K_3(\infty),....,$ require the knowledge of $K_0, K_1, f_0, f_1,$ and f_2. Equation (55) in the limit $\tau \to \infty$, reduces to

$$f_0(\infty,\eta) = \frac{\mu_0}{Sin\,\mu_0} Cos(\mu_0) \quad (58)$$

Then we find f_1 K_1, f_2 *and* K_2. For asymptotically long times, i.e., $\tau \to \infty$, equation (35) and (37) give $K_i's$ *and* $f_k's$ as

$$K_i(\tau) = \frac{\delta_{ij}}{Pe^2} - \beta f_i(\infty,1) - \int_0^h U_f^{'} \; f_{i-1}(\infty,\eta)\,d\eta \qquad (i = 1,2,3,....) \quad (59)$$

$$\frac{\partial^2 f_k}{\partial \eta^2} + \mu_0^2 f_k = (U_f^{'} + K_1) f_{k-1} - \left(\frac{1}{Pe^2} - K_{2I}\right) f_{k-2}, \qquad (k = 1,2,...) \quad (60)$$

The $f_k's$ must satisfy the conditions (32) and this permits the eigen function expansion in the form of

$$f_k(\infty,\eta) = \sum_{j=0}^{9} B_{j,k} Cos(\mu_j \eta),\ k = 1,23,.. \quad (61)$$

Substituting (61) in (60) and multiplying the resulting equation by $\cos(\mu_j \eta)$ and integrating with respect to η from 0 to h, gives

$$B_{j,k}\, Cos(\mu_j \eta) = \frac{1}{\mu_j^2 - \mu_0^2}\left[\frac{1}{Pe^2}\sum_{j=0}^{9} B_{j,k-2} Cos(\mu_j \eta) - U_f{'}\sum_{j=0}^{9} B_{j,k-1} Cos(\mu_j \eta) - \sum_{j=0}^{9} K_{iI} B_{j,k-i} Cos(\mu_j \eta)\right]$$

Multiplying by $Cos(\mu_j \eta)$ and integrating with respect to η, we get

$$B_{j,k} = \frac{1}{\mu_j^2 - \mu_0^2}\left[\frac{1}{Pe^2}\sum_{j=0}^{9} B_{j,k-2} - U_f^{'}\sum_{j=0}^{9} B_{j,k-1} - \left(1 + \frac{Sin\,\mu_j}{2\mu_j}\right)^{-1} \sum_{j=0}^{9} B_{j,k-i}\, I(j,l)\right] \; k = (1,2) \quad (62)$$

where

$$I(j,l) = \frac{1}{h}\int_0^h U' Cos(\mu_j \eta) Cos(\mu_l \eta) d\eta = I(l, j) \quad (63)$$

$$B_{j,-1} = 0, B_{j,0} = 0 \qquad for \;\; j = 1 \;\; to \;\; 9 \quad (64)$$

The first expansion coefficient $B_{0,k}$ in equation (61) using conditions (38) to (41) can be expressed in terms of $B_{j,k}$ (j =1 to 9) as,(Using the boundary condition $\frac{1}{h}\int_0^h f_k(\tau,\eta) d\eta = \delta_{k0} = 0$)

$$B_{0,k} = -\left(\frac{\mu_0}{\sin\mu_0}\right)\sum_{j=0}^{9} B_{j,k} \frac{Sin\,\mu_j}{2\mu_j} \;\; k = (1,2,3,...) \quad (65)$$

Further, from (57) and (61) we find that

$$B_{0,0} = \frac{\mu_0}{Sin\,\mu_0} \quad (66)$$

Using (63), (64) and (66) in the resultant equation after substituting i = 1 in (59), we obtain

$$K_1(\infty) = -\frac{I(0,0)}{\left[1+\frac{Sin\,2\mu_0}{2\mu_0}\right]} \quad (67)$$

Using (62), (63) and (66) in the outcome equation after substituting i = 2 in (59), we obtain

$$K_2 = \frac{1}{Pe^2} - \frac{\sin\mu_0}{\mu_0\left(1+\frac{Sin\,2\mu_0}{2\mu_0}\right)}\sum_{j=0}^{9} B_{j,k-i}\, I_{j,0} \quad (68)$$

where $B_{j,1} = -\frac{1}{\mu_j^2-\mu_0^2}\left(1+\frac{Sin\,\mu_j}{2\mu_j}\right)^{-1}\frac{\mu_0}{Sin\,\mu_0} I(j,0)$

The mean concentration distribution as a function of and the parameters Pe, and is found using the asymptotic coefficients in (32).This distribution is an approximate representation for short and moderate times and is valid for a long duration. By calculating the cross-sectional average from (25) the initial condition for solving (34) may be obtained. According to Sankar Rao (1995), the solution of (34) with asymptotic coefficients may be expressed as follows: Long-term evaluations of the coefficients have an impact that is independent of the initial concentration distribution.

$$\theta_m(\tau, X) = \frac{1}{2Pe\sqrt{\pi K_2(\infty)\tau}}\exp\left[K_0(\infty)\tau - \frac{\left[X+K_1(\infty)\tau\right]^2}{4K_2(\infty)\tau}\right] \quad (69)$$

where $\theta_m(\tau,\infty) = 0,\ \frac{\partial\theta_m}{\partial X}(\tau,\infty) = 0$

4. Results and Discussion

The effects of magnetic field, electric field, and heterogeneous chemical reactions on the dispersion of a solute in a Bingham fluid (blood) as it flows through a porous medium in a rectangular channel enclosed by porous beds are examined. The channel walls act as catalysts for the reaction. Figures 2 to 18 show the graphic representation of the most dominant dispersion coefficient, convection coefficient, and mean concentration for fixed values using MATHEMATICA 12.0. These values are calculated for different values of Hartmann number(M=1,1.1,1.2,1.3), porous parameter $(\sigma = 10,60,100,120)$, rheological parameter $(\eta_c = 0,0.1,0.2,0.3)$, reaction rate parameter $(\beta = 10^{-2}, 1, 10^2)$ and electric number(We=5, 15,25,35) for fixed values $X_s = 0.019, X = 0.1, Pe = 100, \alpha = 0.10$.

Equation (57), which is used to numerically assess the expression for the absorption coefficient $-K_0(\infty)$, is displayed in Figure 2. Although it is unaffected by the Hartmann number, porous parameter, rheological parameter, it is clear that the increases as the wall reaction parameter β grows. Molecular diffusion can provide the reaction at the wall more quickly if the absorption parameter takes huge values. Therefore, compared to tubular flow, there is greater solute absorption at the annulus wall.

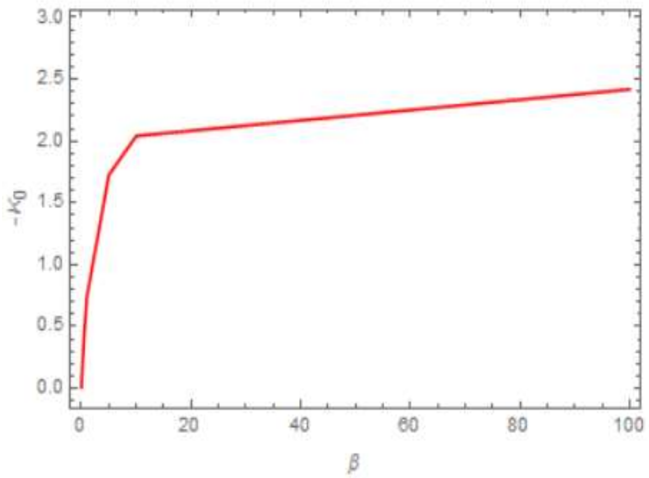

Figure 2: Variation of $-K_0$ versus β

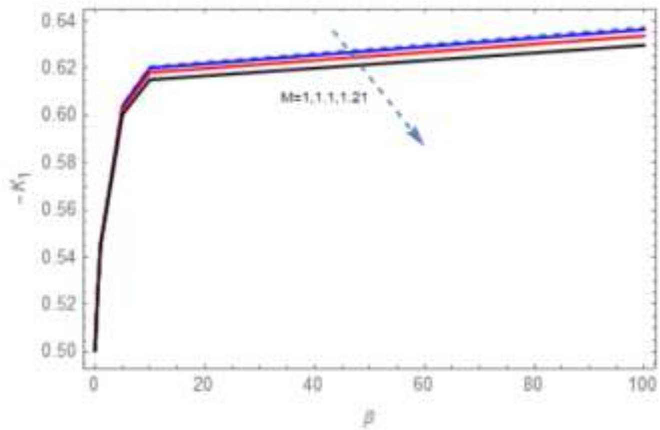

Figure 3: Impact of M on $-K_1$

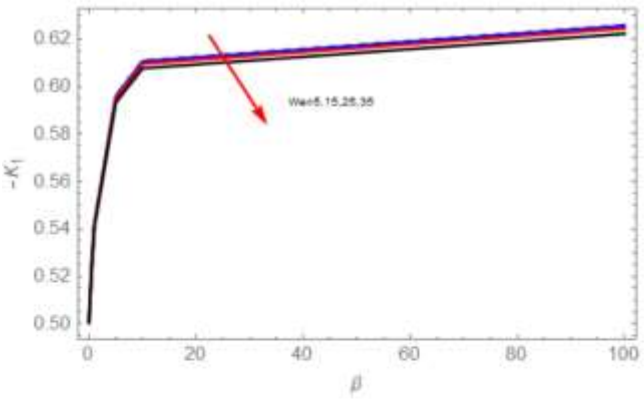

Figure 4: Impact of We on $-K_1$

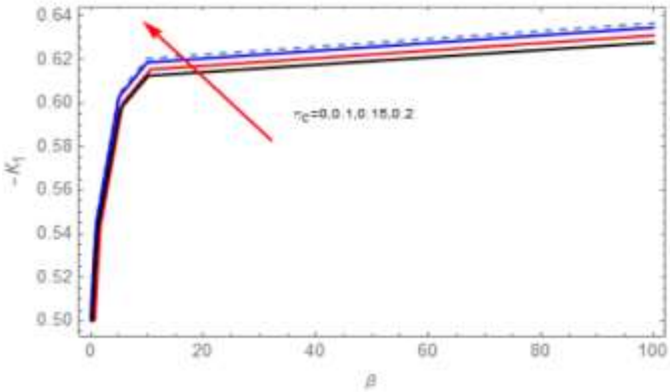

Figure 5: Impact of η_c on $-K_1$

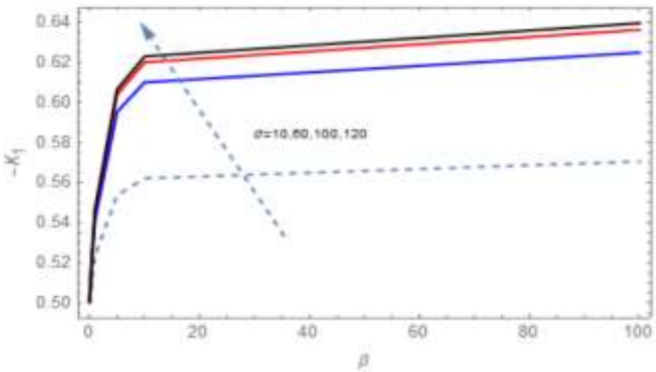

Figure 6: Impact of σ on $-K_1$

The variance of the convection and dispersion coefficients diminishes as the range of the wall reaction parameter β grows as seen in Figures 3 to 10. This phenomenon is attributed to the synergistic effect of magnetic field strength and wall reaction parameter, enhancing the decline in convection and dispersion coefficients (Singh, J., and Kumar, V. (2020)). Figures 3 to 6 display the convection coefficient expression for different values of the Hartmann number, electric number, rheological parameter, and porous parameter with wall response parameter. These expressions are numerically analysed using equation (67). It is observed that the convection coefficient decreases with increases in the Hartmann number and electric number. The increase in Hartmann number and electric number enhances the convection coefficient in blood flow due to the augmented Lorentz force, electrical body force, and porous medium resistance, which intensify the flow velocity and mixing, thereby increasing dispersion(Tripathi and Kumar(2020)). Figures 5 and 6 show that the increase in rheological parameter and porous parameter, result in increasing convection coefficient $-K_1(\tau)$.As a result, the laminar flow is maintained.

The expression for the dispersion coefficient is shown in Figures 7 to 10 for varies values of the rheological parameter, electric number, Hartmann number, and porous parameter with values of the wall response parameter. It is evaluated numerically using equation (68).

Increasing the Hartmann number and promoting plug flow conditions in blood flow typically reduce the dispersion coefficient in Figure 7 and 8. The Hartmann number quantifies the influence of magnetic fields on electrically conducting fluids; higher values suppress velocity fluctuations, leading to more uniform flow and decreased mixing. Plug flow, characterized by a uniform velocity profile across the cross-section, minimizes axial dispersion by ensuring that fluid elements move together without significant mixing. Consequently, both increased Hartmann numbers and plug flow conditions tend to reduce the dispersion coefficient in blood flow. The former impact outweighs the latter for all η due to the two-dimensional structure of the flow in a channel, and we see a monotonic drop in $K_2(\tau) - Pe^{-2}$ as η_c increases. When $\eta_c = 0,(68)$ gives Annapurna and Gupta(1979). Plotting the dispersion coefficient versus reaction rate parameter values is shown in Figures 9 and 10. It is found that when the electric number and porous parameter increases, the dispersion coefficient rises. This is because higher electric fields and porosity promote more irregular flow paths and enhanced mixing, causing increased dispersion of solutes within the blood.

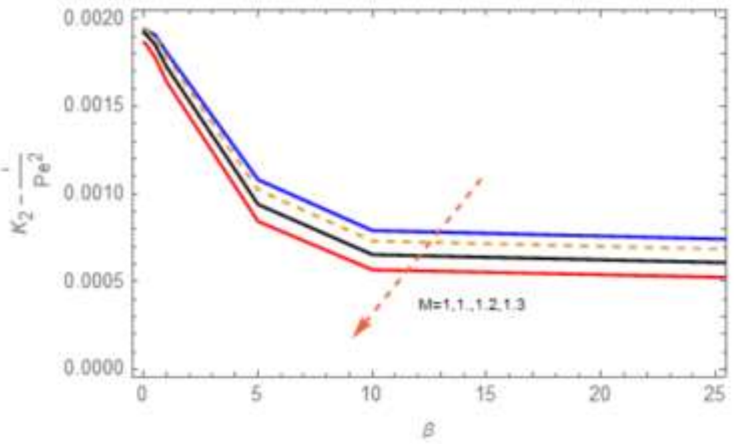

Figure 7: Impact of M on $K_2(\tau) - Pe^{-2}$

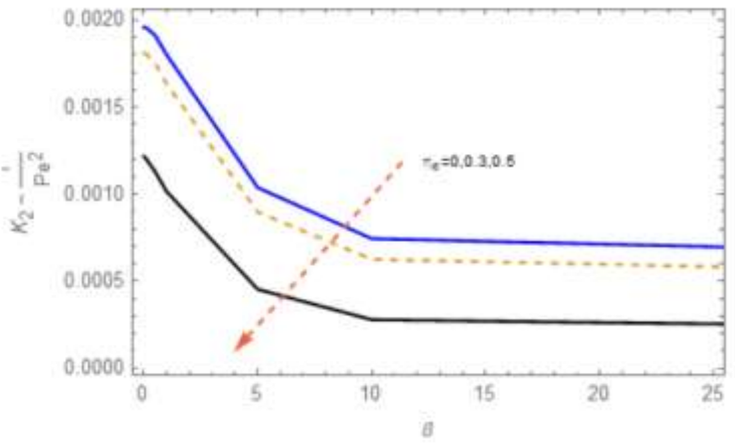

Figure 8: Impact of η_c on $K_2(\tau) - Pe^{-2}$

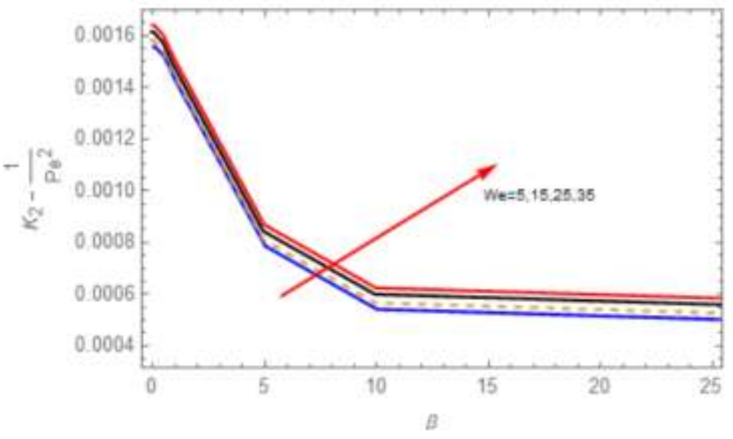

Figure 9: Impact of We on $K_2(\tau) - Pe^{-2}$

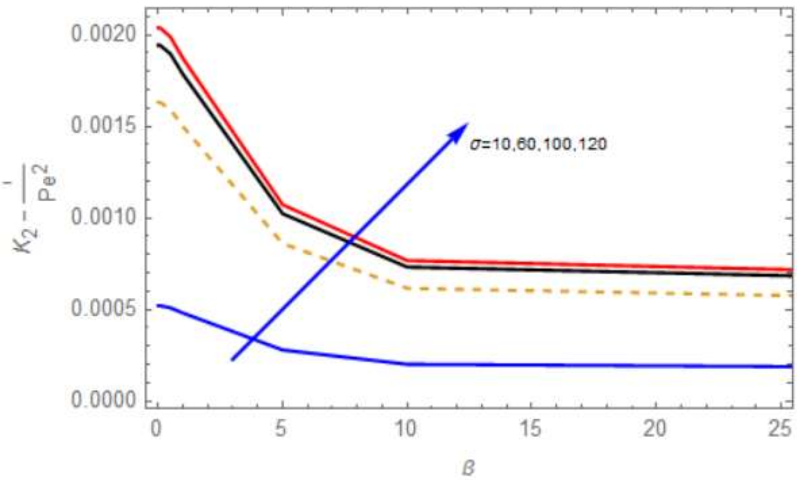

Figure 10: Impact of σ on $K_2(\tau)-Pe^{-2}$

Figures 11 to 15 depict the mean concentration θ_m with time for different values of Hartmann number, electric number, reaction rate parameter, rheological parameter and porous parameter. Figure 11 to 13 shows that decrease in θ_m with increasing the value of Hartmann number, reaction rate parameter and porous parameter. This phenomenon occurs due to the enhanced Lorentz force, which reduces the flow velocity and increases the residence time of the solute, leading to increased reaction and reduced mean concentration. Figure 14 and 15 show the plots of time dependent mean concentration versus for different values of electric number and rheological parameter. It is observed that the mean concentration increases with increasing electric number and rheological parameter, but it is reverse while increasing time. Figures 16 to 18 depict the mean concentration θ_m with X for different values of Hartmann number, rheological parameter and porous parameter.

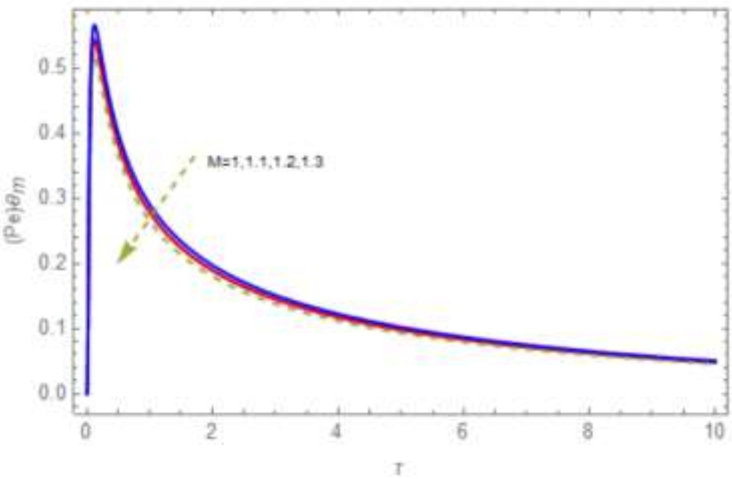

Figure 11: Impact of M on θ_m

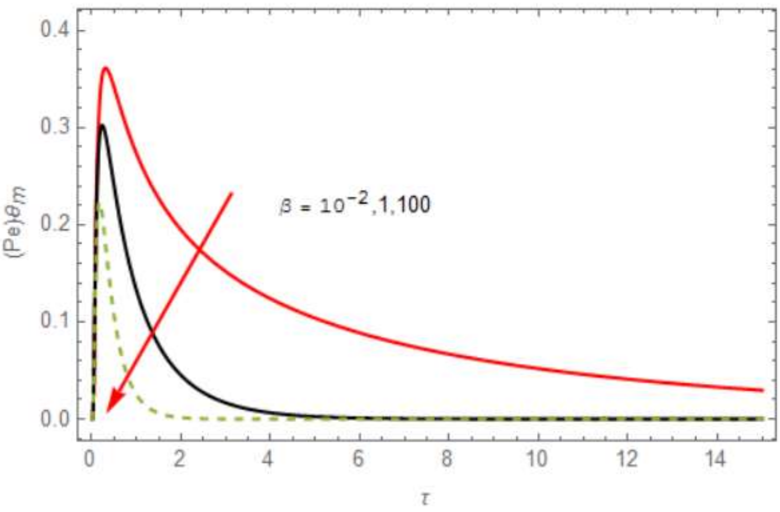

Figure 12: Impact of β on θ_m

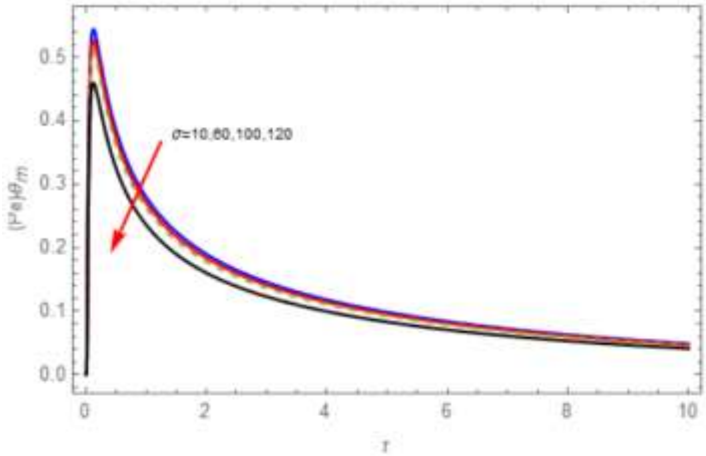

Figure 13: Impact of σ on θ_m

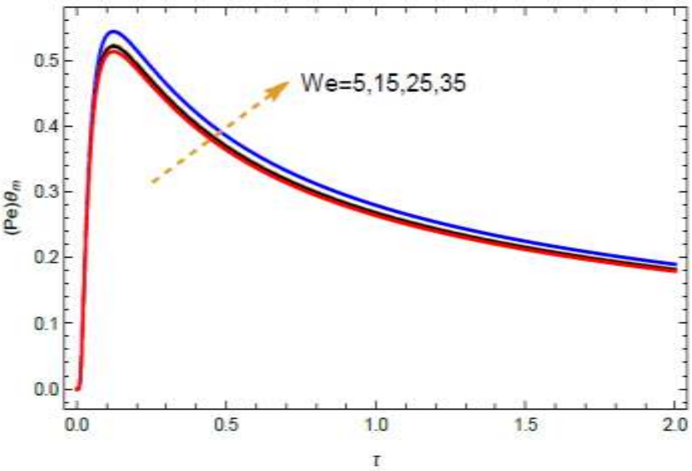

Figure 14: Impact of We on θ_m

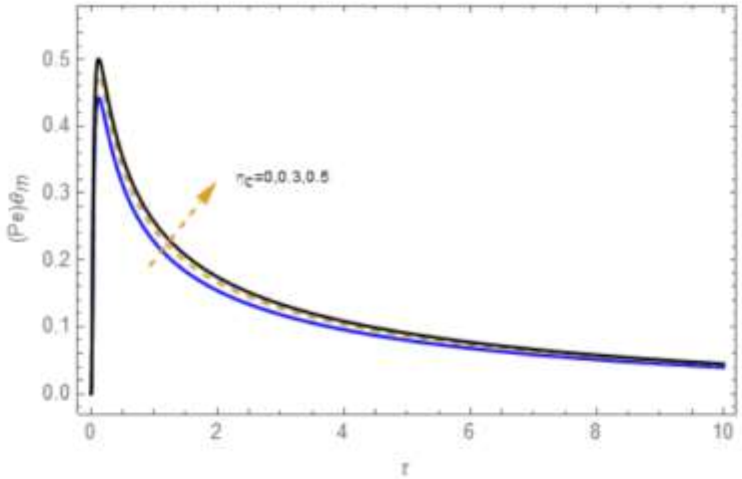

Figure 15: Impact of η_c on θ_m

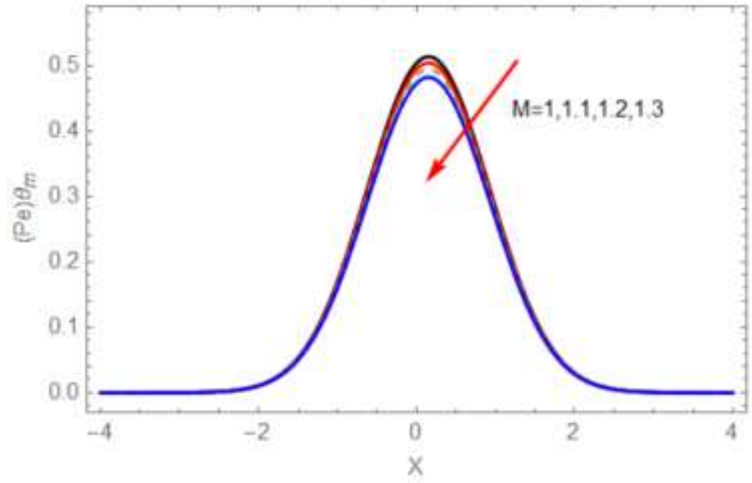

Figure 16: Impact of M on θ_m

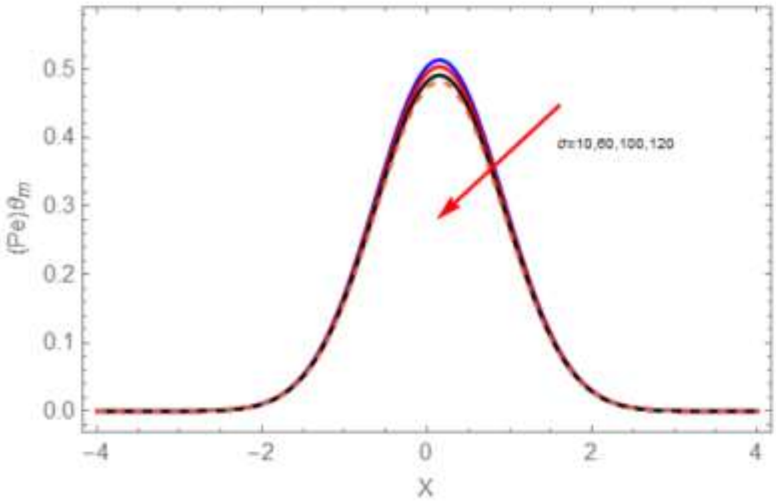

Figure 17: Impact of σ on θ_m

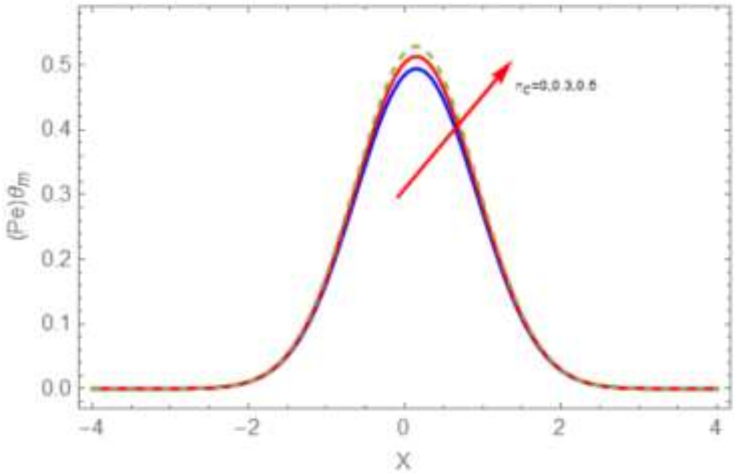

Figure 18: Impact of η_c on θ_m

Figure 16 and 17 shows that decrease in peak of θ_m with increasing the value of Hartmann number and porous parameter. This can lead to a more uniform distribution of solutes, resulting in a higher peak mean concentration. From Figure 18 it is evident that increase in θ_m with increasing the value of rheological parameter. When the breadth of the channel or rheological parameters (like viscosity) increase, the peak of mean concentration in blood flow increases. A wider channel allows for more dispersion of the solute, leading to a more uniform distribution and a lower peak concentration.

5.Conclusion

The generalised dispersion model of Sankarasubramanian and Gill (1973) is used to examine how a magnetic field affects a solute dispersion in a fluid flow with wavy boundary retention effects in a conduit. The three transport coefficients the exchange (absorption) coefficient, convection coefficient, and dispersion coefficient are used to characterise the dispersion process. It is observed that the absorption coefficient is unaffected by the rheological parameter, electric number, Hartmann number, and porous parameter. Both the electric number and the magnetic field affect the convection coefficient. It is found that as the electric number and magnetic field grow, the negative asymptotic convection coefficient drops, whereas as the wall absorption parameter increases, it increases. The boundary reaction dramatically reduces the axial dispersion.This results corresponds to those given by Ashis Kumar Roy et al., (2018).

Table 1 Equation roots for $\mu_n \tan \mu_n = \beta$

β	μ_0	μ_1	μ_2	μ_3	μ_4	μ_5	μ_6	μ_7	μ_8	μ_9
10^{-2}	0.099834	3.14477	6.28478	9.42584	12.5672	15.7086	18.8501	21.9916	25.1331	28.2747
0.05	0.22176	3.15743	6.29113	9.43008	12.5703	15.7111	18.8522	21.9934	25.1347	28.2761
10^{-1}	0.311053	3.1731	6.29906	9.43538	12.5743	15.7143	18.8549	21.9957	25.1367	28.2779
0.5	0.653271	3.29231	6.36162	9.47749	12.606	15.7397	18.876	22.0139	25.1526	28.292
1.0	0.860334	3.42562	6.4373	9.52933	12.6453	15.7713	18.9024	22.2126	25.1724	28.3096
5.0	1.31384	4.03357	6.9096	9.89275	12.9352	16.0107	19.1055	22.2126	25.3276	28.4483
10.0	1.42887	4.3058	7.22811	10.2003	13.2142	16.2594	19.327	22.4108	25.5064	28.6106
100.0	1.55525	4.66577	7.77637	10.8871	13.9981	17.1093	20.2208	23.3327	26.445	29.5577

REFERENCES

Annapurna, N. and Gupta A. S.,(1979).Exact analysis of unsteady m.h.d. convective diffusion Proc.R.Soc.Lond.A. 367, 281-289**.**https://doi.org/10.1098/rspa.1979.0088.
Ashis Kumar Roy, Apu Kumar Saha, Sudip Debnath, (2018), Unsteady Convective Diffusion with Interphase Mass Transfer in Casson Liquid, Periodica Polytechnica Chemical Engineering, 62(2), pp. 215-223, 2018,https://doi.org/10.3311/PPch.10328.

Beavers G.S. and Joseph D.D., 1967.Boundary conditions at a naturally permeable wall. J.Fluid Mech., Vol.30, 197-207.

Cooney D.O., (1976), Biomedical Engineering Principles: An Introduction to Fluids, Heat and Mass transport Processes, First edition, Marcell Dekker, New York.

Gill W.N., and Sankarasubramanian R., 1970. Exact analysis of unsteady convective diffusion, Proc. Roy. Soc. London, A 316, 341-350.

Jayaraman G., Lautier A., Bui-Mong Hung, Jarry G. and Laurent D., (1981), Numerical scheme for modelling oxygen transfer in tubular oxygenators, Medical & Biological Engineering & Computing,19, 524-534.

Lightfoot E.N., (1974), Transport phenomena in living system, JohnWiley and Sons, New York.

Middleman S., (1972), Transport phenomena in the cardiovascular system, Sixth edition iley Interscience, Chapter 3, 118.

Misra J.C., and Adhikary S.D.,2017, Flow of a Bingham fluid in a porous bed under the action of a magnetic field: Application to magneto-hemorheology, Engineering Science and Technology, an International Journal, 20, 973–981.http://dx.doi.org/10.1016/j.jestch.2016.11.008.

Nirmala P. Ratchagar and Vijaya Kumar, (2015). Exact analysis of Unsteady Convective Diffusion for Blood Flow with Interphase Mass Transfer In Magnetic Field,Bangmod Int. J. Math. & Comp. Sci.1(1), 63- 81.

Rudraiah.N., Mallika K.S and Sujatha N.(2016). Electrohydrodynamic Dispersion with Interphase Mass Transfer in a Poorly Conducting Couple Stress Fluid Bounded by Porous Layers, Journal of Applied Fluid Mechanics, Vol. 9, No. 1, 71-81.

Sankara R.,(1995), Introduction to Partial Differential Equations, Third edition, Prentice Hall of India.

Sakarasubramanian, R. and Gill, W.N.(1973). Unsteady convective diffusion with interphase mass transfer. Proc. Roy. Soc. London, A 333, 115-132.
Siddheshwar, P.G., S. Manjunath and Sripad (2000). Effect of interphase mass transfer on unsteady convective diffusion: Part I, Plane-Poiseuille flow of a power law fluid in a channel. Chemical Engineering Communications. 180(1):187-207.DOI:10.1080/00986440008912208
Singh, J., & Kumar, V. (2020). Numerical study of electric field effects on synovial fluid dynamics. Journal of Biomechanics, 98, 109433.

Siti Nurul Aifa Mohd Zainul Abidin, Nurul Aini Jaafar and Zuhaila Ismail.(2024), Mathematical analysis of unsteady solute dispersion in Herschel-Bulkley fluid with interphase mass transfer, AIP Conf. Proc. 3128, 020002.https://doi.org/10.1063/5.0215017

Tripathi, D., & Kumar, V. (2020). Electrokinetic effects on blood flow through a narrow channel. Journal of Fluids Engineering, 142(10), 101202.

Taylor G.I., (1953), Dispersion of soluble matter in solvent flowing slowly through a tube, Proceedings of the Royal Society of London A., 219(1137), 186-203.

Taylor G.I.,(1954), Conditions under which dispersion of a solute in a stream of solvent can be used to measure molecular diffusion, Proceedings of the royal society A, 225, 473-477.